Raman spectroscopy study of atherosclerosis in human carotid artery

Grazielle V. Nogueira
Landulfo Silveira, Jr.
Airton A. Martin
Renato A. Zângaro
Marcos T. T. Pacheco
University of Vale do Paraíba-UNIVAP
Institute of Research and Development
Av. Shishima Hifumi, 2911
São José dos Campos
SP, Brazil, 12244-000

Maria C. Chavantes
Carlos A. Pasqualucci
University of São Paulo
Department of Cardiovascular Pathology
Av. Dr. Arnaldo, 455
São Paulo
SP, Brazil, 01246-903

Abstract. Fourier-transform (FT)-Raman spectroscopy has been used for identification and evaluation of human artherosclerotic lesions, providing biochemical information on arteries. In this work, fragments of human carotid arteries *postmortem* were analyzed using a FT-Raman spectrometer operating at an excitation wavelength of 1064 nm, power of 200 mW, and spectral resolution of 4 cm^{-1}. A total of 75 carotid fragments were spectroscopically scanned and FT-Raman results were compared with histopathology. Discriminant analysis using Mahalanobis distance was applied over principal components scores for tissue classification into three categories: nonatherosclerotic, atherosclerotic plaque without calcification and with calcification. Nonatherosclerotic artery, atherosclerotic plaque, and calcified plaque exhibit spectral signatures related to biochemicals presented in each tissue type, such as bands of collagen and elastin (proteins), cholesterol and its esters, and calcium hydroxyapatite and carbonate apatite, respectively. Spectra of nonatherosclerotic artery were then classified into two groups: normal and discrete diffuse thickening of the intima layer (first group) and moderate and intense diffuse thickening of the intima layer (second group). FT-Raman could identify and classify the tissues found in the atherosclerotic process in human carotid *in vitro* and had the ability to identify alterations to the diffuse thickening of the intima layer and classify it depending on the intensity of the thickening.
[DOI: 10.1117/1.1908129]

Keywords: biological tissues; *in vitro* spectroscopy; diagnostic algorithm; discriminant analysis; intima thickening; Raman spectroscopy

Paper JBO-002503 received Jun. 22, 2004; revised manuscript received Jan. 18, 2005; accepted for publication Jan. 18, 2005; published online May 23, 2005.

1 Introduction

Atherosclerosis, a stenotic lesion of arterial walls is a leading cause of death affecting almost one third of humans in developed countries.[1] Evolution of atherosclerosis follows well-defined steps, including the progressive thickening of the arterial intima layer due to cellular proliferation (foam cells), lipid and cholesterol intracellular deposition, extracellular lipid accumulation, with change in the musculoelastic layer and enlargement of the upper intima (''collagenous cap'') leading to a fibroatheroma plaque.[2] In advanced lesions lipid and necrotic deposits accumulate within the intima and calcium crystal build-up takes place (calcification of artery wall).[3] Physician's intervention usually occurs when the plaque is symptomatic, with high commitment of important organs, such as heart and brain. Some researchers believe that instead of volume or area the plaque content is more effective to prevent plaque evolution and management of disease evolution.[4]

The interest in using laser spectroscopy for atheromatous plaque identification and quantification has been increasing. One of the first attempts to use laser spectroscopy for diagnosis of plaque content was made by Kittrell et al.,[5] in which an excitation wavelength of 480 nm was used to induce autofluorescence in atherosclerotic aorta. They demonstrated that fluorescence emission from normal arteries was significantly different from fibrous plaque. Initially researchers were focused on autofluorescence emission for tissue characterization, aiming at its use as a laser angioplasty guidance system.[6–9] However, due to the little biochemical information carried out by fluorescence spectrum the use of Raman spectroscopy for biological tissue analysis has been evidenced.[10–12]

The Raman spectroscopy is an optical tool which could permit less invasive and nondestructive analysis of biological samples, allowing one to get precise information on biochemical composition from different types of human tissues, such as coronary arteries,[13,14] lung,[15] and colon,[16] that can be combined with optical cables for excitation and detection of Raman signals without tissue removal. The longer wavelengths used in the Fourier-transform Raman (FT-Raman) systems reduce the effects of tissue fluorescence, promoting less photolytic degradation of samples occurring due to the longer

Address all correspondence to Professor Dr. Landulfo Silveira, Jr. Tel: (55)(12)3947-1124; Fax: (55)(12)3947-1149; E-mail: landulfo@univap.br

1083-3668/2005/$22.00 © 2005 SPIE

wavelength laser, this allows for higher powered laser to be used.

The process of Raman scattering can be viewed as an inelastic phenomenon in which the scattered photon is shifted in frequency from the incident photon as it either gains energy from or loses energy to a particular vibrational mode of the molecule. Thus, Raman spectroscopy can be used to access the molecular constitution of a specific tissue and then classify it according to differences observed in the spectra.[14]

Principal components analysis (PCA), a multivariate statistical tool, has been applied with success in spectral analysis of biological samples, detecting spectral alterations that occur after changes in the morphology and physiology of biological tissues. Within a set of spectral data, there are usually many different variations that make up a particular spectrum. Background, differences in constituents, instrument variations, sample handling, and others affect the appearance of the final spectrum. Yet with several changes occurring at the same time, there are only a few independent variables accounting for all spectral differences. Normally, the largest variation in the spectral data is due to differences in the constitution of the samples, a few variables. One can achieve simplification of information redundancy or reduction of variables by using PCA. PCA extracts the relevant information from the original data (A) and generates a new set of variables, called principal components (PC) and scores (S). The PC are related to the most important variation of all spectra; first PC account for most of the variation of the data, the last ones carry only noise, and S are related to the weight of each PC to reconstruct the original data[17]

$$A = S \times \mathrm{PC}, \tag{1}$$

where A is an m by n matrix of Raman spectra (m = wave number, n = number of spectra), S is the n by n matrix of reconstruction scores, and PC is an n by m matrix of principal components vectors. Since S is the weight, meaning the importance of each PC to form the original spectrum, and the PC carries spectral information in the form of defined peaks and valleys, it could be used to build an algorithm based on the PCA scores to classify samples into well-defined categories depending of the histopathological findings and the occurrence of Raman features.

PCA has been used for statistical analysis and classification in a variety of human diseases, such as near-infrared fluorescence spectroscopy of Alzheimer disease,[18] near-infrared Raman spectroscopy of cervical precancer analysis,[19] human breast cancer analysis,[20] and skin.[21] Recently, Deinum et al.[12] and Silveira, Jr. et al.[14] showed that PCA combined with logistic regression and Mahalanobis distance, respectively, could be used as a classification tool for *in vitro* analysis of atherosclerotic coronary artery samples, with high sensitivity.

The Mahalanobis distance (also called m distance) is a very useful way to find the similarity of a set of values from one group of samples compared to another group for discriminant analysis. The m distance (D^2) is calculated as follows:

$$D_i^2 = (x - \mu_i)^T V^{-1} (x - \mu_i), \tag{2}$$

where i denotes the known sample group number, x is the vector of the sample parameter, μ is the mean vector for the specific group, and V is the covariance matrix of the group.

The m distance has advantages over Euclidean distance because it takes not only the relative distance from the sample to the mean of the group but also takes into account the covariance matrix of the data.[22] It means that m distance gives a statistical of how well the sample matches the grouped data. According to the Eq. (2) high m distance means better group separation. The m distance can be used to classify the sample into well-defined classes.

The primary objective of the present work is to verify if FT-Raman spectroscopy, compared to histopathological analysis as a gold standard, is capable of identifying and classifying the different types of tissues found in the atherosclerotic process of human carotid artery *postmortem*, using an algorithm based on the results of PCA and m distance applied over all spectra. Moreover, the secondary objective of this work is to observe if the PCA algorithm is able to identify such alterations in the nonatherosclerotic artery wall, with respect to the diffuse thickening of the intima layer, and classify it depending on the intensity (severity) of the thickening.

2 Materials and Methods

2.1 *Human Carotid Artery Samples*

Carotid artery samples were obtained from the Autopsy Service at the University of São Paulo (São Paulo, SP, Brazil) taken from cadavers without prior knowledge of *causa mortis*. After extracting carotid artery segments approximately 50 mm in length from 22 subjects, they were snap-frozen and stored in liquid nitrogen ($-196\,^{\circ}\mathrm{C}$) prior to use. At the moment of Raman spectral analysis the samples were unfrozen with 0.9% saline solution to reach room temperature. Segments were cut in 10×10 mm fragments and placed in an anodized aluminum sample holder. A total of 75 fragments were spectroscopically scanned. This protocol was approved by the Ethics Committee of the University of Vale do Paraíba under No. L014/2003/CEP.

2.2 *Raman Spectra Collection*

FT-Raman spectra were obtained using a spectrometer (model RFS 100/S, Bruker Inc., Karlsruhe, Germany) that uses a Nd:yttrium–aluminum–garnet laser at 1064 nm operating wavelength and 200 mW of excitation power. Spectra were obtained with 250 scans, with collection time of approximately 8 min under a spectrometer resolution of 4 cm^{-1}. After spectroscopic scanning, the spot where the laser illuminated the tissue was marked with India ink and the fragment was immersed in 10% formalin solution, bottled, and labeled for histopathological studies.

2.3 *Histopathological Analysis*

Traditional histopathological technique was performed. Hematoxilin and eosin, Verhoeff, Masson, and Picrossirius staining were used for tissue structure observation and Sudan staining was used for fat deposit identification. The histopathological classification was done by a board-certified pathologist according to the Committee on Vascular Lesions Report.[23] Based on these results the samples were then classified into three main tissue types: (a) nonatherosclerotic (normal and intimal thickening); (b) atherosclerotic plaque without calcification; and (c) atherosclerotic plaque with calcification.

The fragments classified as nonatherosclerotic were subdivided into four categories: (1) normal, (2) discrete diffuse thickening of the intima layer, when thickening represented up to 1/3 of the media layer thickness, (3) moderate diffuse thickening of the intima layer, when thickening represented from 1/3 to 1/2 of the media layer thickness, and (4) intense diffuse thickening of the intima layer, when thickening represented more than 1/2 of the media layer thickness.

2.4 *FT-Raman Spectral Analysis—Algorithm Based on PCA*

All spectra were recorded in binary format and converted to ASCII format for postprocessing. In order to prepare the data to perform PCA, all spectra were normalized using the most intense peak in the region of 800–1800 cm^{-1} to obtain scale-free intensity data.

In order to develop an algorithm for tissue classification, the FT-Raman spectra were analyzed through PCA technique. The PC and *S* were obtained from all 75 spectra using a routine written in Matlab© software (The Mathworks, Inc., CA) with the NIPALS-PCA algorithm.[17] Since *S* are the weight, or the importance of each PC to form the original spectrum, they can be used to build an algorithm to correlate the histopathological findings to FT-Raman features.

PCA analysis was performed in two ways. First the PC and *S* were calculated of all the 75 spectra to classify tissues in (a) nonatherosclerotic (NA), (b) atherosclerotic without calcification (NC), and (c) atherosclerotic with calcification (*C*). After, the PC and *S* were calculated using only the 48 spectra of the histopathologically nonatherosclerotic group. Using this approach the nonatherosclerotic tissues were classified as (1) normal and discrete diffuse thickening of the intima (N + DTh) and (2) moderate and intense diffuse thickening of the intima (MTh + ITh). The discriminator among all histopathological groups was Mahalanobis distance, that has the advantage to the Euclidean distance because uses the covariance of the data. M distance calculations were done using Matlab Statistics toolbox.

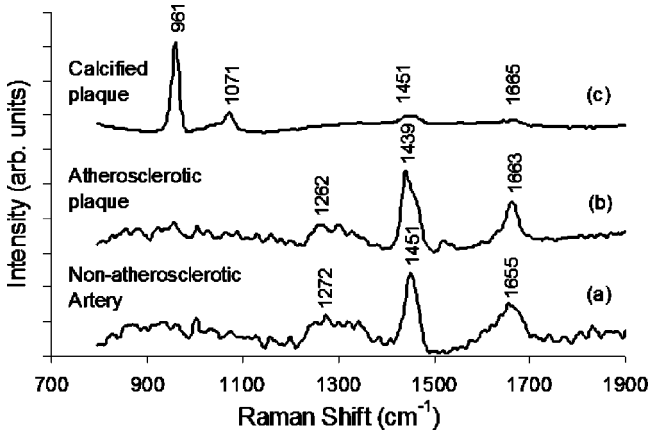

Fig. 1 FT-Raman spectra of *in vitro* human carotid artery: (a) nonatherosclerotic artery; (b) atherosclerotic plaque without evidence of calcification; (c) atherosclerotic plaque with prominent calcification.

3 Results

3.1 *Histopathological Results*

Of the 75 fragments of carotid histopathologically analyzed, 20 were classified as normal, 17 presented a discrete thickening, 7 with moderate thickening, and 4 with intense thickening of the intima layer. A total of 19 fragments were classified as atherosclerotic tissues without evidence of calcification and 8 were classified as atherosclerotic with calcification.

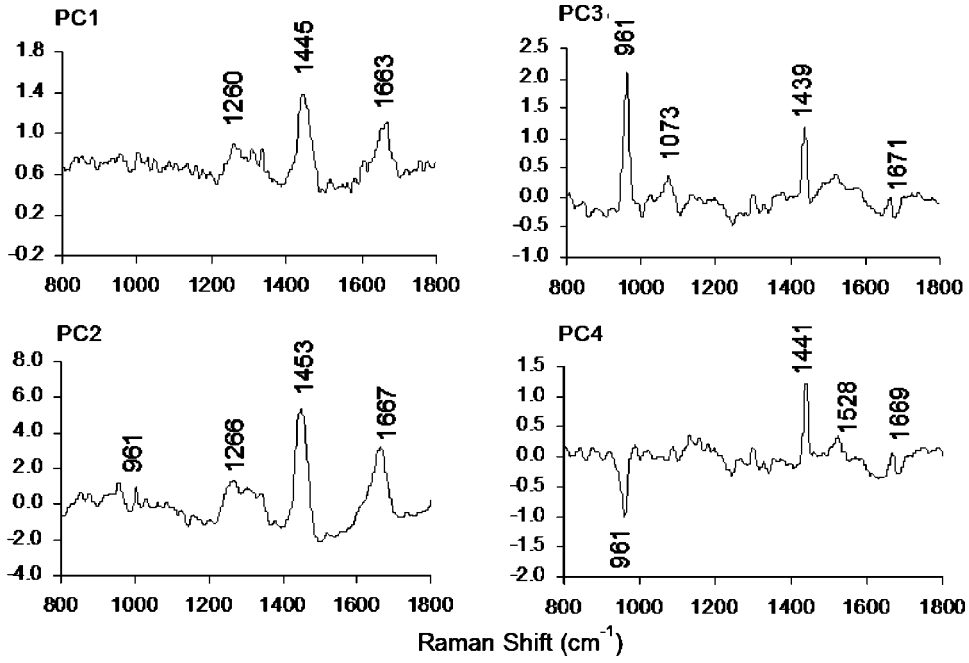

Fig. 2 Spectra of the first four PC vectors calculated using 75 FT-Raman spectra. Labeled features represent main peaks of each PC that can be related to Raman bands found in carotid arteries.

3.2 *Spectral Features*

Typical FT-Raman spectra of *in vitro* human carotid artery walls are shown in Fig. 1. A Raman spectrum shows vibrational bands from biomolecules and can reveal the composition of the artery wall. The FT-Raman spectrum of normal coronary tissue is shown in Fig. 1(a). Most important bands are assignable to structural proteins, mainly collagen and elastin. Observed predominant bands at 1655, 1451, and 1272 cm^{-1} are due to amide I, C–H bending, and amide III vibrations of structural proteins, respectively.[14,24,25] The presence of protein peaks at normal tissue could indicates that the spectrum comes probably from extracellular matrix in the media layer, and the intima contribution to spectrum can be negligible. Raman spectrum of atheromatous plaque [Fig. 1(b)] exhibits bands assignable to cholesterol and its esters with major bands at 1439 and 1663 cm^{-1}.[14,24,25] The most significant differences among normal and atheroma spectra are observed in the C–H bending because in normal tissues the peak appears in 1451 cm^{-1} and in atheormatous tissues this peak has a frequency shift appearing in 1439 cm^{-1}. This shift can be related to the accumulation of lipids in the atheromatous plaque. This lipid deposits can also be observed in the peak related to vibrational mode of amide I where in the normal tissue it appears in 1655 cm^{-1} and in the atherosclerotic tissue in 1663 cm^{-1}. Although atherosclerotic fibrous cap can show the protein contribution to the spectrum of some atherosclerotic samples, the lipid core is mainly composed of fat and cholesterol, overlapping the 1451 cm^{-1} band of normal tissue.[14] Calcified atheromatous plaques show a very distinct Raman feature with main bands at 961 and 1071 cm^{-1} due to phosphate and carbonate symmetric stretching vibrations of accumulated calcium hydroxyapatite and carbonateapatite respectively [Fig. 1(c)].[14,24,25]

3.3 *Principal Components Analysis*

Each PC has a single axis in space and one is perpendicular to the other. When each observation (spectrum) in each PC is projected, new variables come up, the scores *S* (orthonormals in respect to each other). Since the scores represent the intensity of each PC in the spectrum, they can be plotted as they do not carry redundant information.

The results of our calculation show that the first four PCs represent more than 99% of all spectral variation. PC1 represents 80% of such variation and the remaining PCs contribute with about 19%. Analyzing Fig. 2 it was observed that the highest spectral differences between the three types of human carotid arteries can be found in the PC2 and the PC3 (i.e., peaks in 961, 1439, and 1453 cm^{-1}), showing the presence of relevant peaks in the same positions as the tissue spectra and therefore they were used for the diagnostic algorithm. PC1 [Fig. 2(a)] does not carry any additional information that could be used for diagnosis, since it reproduces the average spectrum. PC2 [Fig. 2(b)] brings the entire spectral feature from the original data, whereas PC3 [Fig. 2(c)] shows the main features for the atherosclerotic and calcified tissue. Although PC4 [Fig. 2(d)] has negative as well as positive feature it does not bring additional information from PC3.

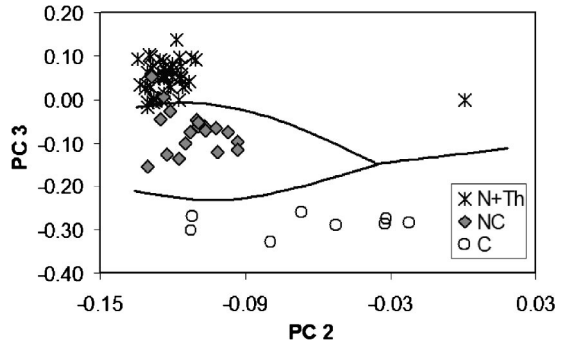

Fig. 3 Scatter plot of the second and third PC scores calculated using 75 FT-Raman spectra of carotid arteries. N+Th represent samples of histopathologically normal and diffused thickening of the intima, NC represents the atherosclerotic plaque without calcification, and *C* represents the calcified plaque. Black line represents Mahalanobis-based classification surface.

3.3.1 *Diagnosis of atherosclerosis applied to all 75 spectra*

Figure 3 shows the scatter plot of PC2 versus PC3 evidencing differences in scores among the three types of tissues. Two diagnostic (discriminant) lines based on the Mahalanobis distance were drawn aiming for the best separation of three categories. A total of 46 out of 48 normal arteries were classified as NA, 17 out of 19 atheromatous plaques were classified as NC, and 8 out of 8 calcified plaques were classified as *C*.

Table 1 Results from tissue histopathology compared to Raman diagnostic algorithm and correspondent sensitivity/specificity values. NA—nonatherosclerotic carotid artery; NC—atherosclerotic plaque without calcification; *C*—atherosclerotic plaque with calcification.

	PCA diagnosis					
	NA	NC	*C*	Total	Sensitivity (%)	Specificity (%)
Histopathological diagnosis						
Nonatherosclerotic	46	2	0	48	96	93
Atherosclerotic plaque without calcification	2	17	0	19	89	96
Atherosclerotic plaque with calcification	0	0	8	8	100	100

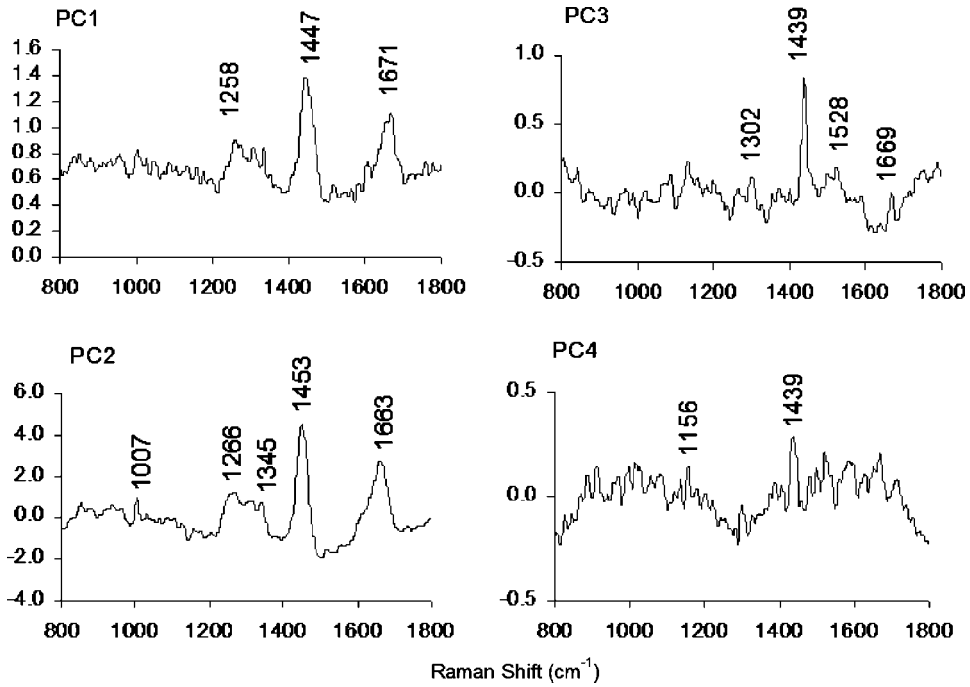

Fig. 4 Spectra of the first four PC vectors calculated using 48 spectra of nonatherosclerotic tissues. Labeled features represent main peaks of each PC related to Raman bands of normal human carotid arteries.

Diagnostic algorithm's sensitivity and specificity indices were calculated as described by Weiss[26] for each one of the tissue categories. These results are summarized in Table 1.

3.3.2 *Diagnostic algorithm applied to 48 spectra of nonatherosclerotic samples*

Histopathological findings indicated that most of the normal arteries were basically nonatherosclerotic intimal thickening. In order to develop an algorithm to identify this thickening using the FT-Raman spectra, the PCA was calculated using only the 48 nonatherosclerotic spectra. Now, the first four PC represented about 90% of all spectral variations. Figure 4 states that the majority of the spectral characteristics of nonatherosclerotic spectra, as has occurred using all non- and atherosclerotic spectra, was found in PC2 and PC3. Figure 5 shows the scatter plot of the scores of PC2 versus PC3 distinguishing two tissue categories: (1) normal and discrete diffuse thickening of the intima layer (N+DTh) and (2) moderate and intense diffuse thickening of the intima layer and (MTh +ITh). The line represents Mahalanobis-based classification for best group separation.

Observing the dispersion graph of the 37 spectra of the group (N+DTH), 32 correctly had been classified by the PCA if compared with the results gotten for the histopathological analysis and of the 11 spectra previously classified as pertaining to the group (MTH+ITH), 8 had found agreement in the classification, seen in Table 2. Sensitivity and specificity indices for the diagnostic of nonatherosclerotic intimal thickening were calculated and also are shown in Table 2.

4 Discussion and Conclusion

In this work an algorithm has been developed for *in vitro* diagnosis of atherosclerosis in human carotid arteries using FT-Raman spectra collected from fragments *postmortem* with the spectral analysis performed by PCA. The PCA scores showed to be efficient in discriminating among the three types of tissues, nonatherosclerotic (normal+intimal thickening), atherosclerotic plaque without calcification, and atherosclerotic plaque with calcification. The sensitivity and specificity for the nonatherosclerotic tissue was 96% and 93%, respectively. The sensitivity for atherosclerotic plaque and calcified plaque diagnosis was very high, about 89% and 96% respectively, and specificity was about 100% for both. It was found that 71 out of 75 samples (94%) could be correctly classified when compared with histopathology (gold standard). Comparable results were obtained by Silveira, Jr. et al.,[14] where 111 fragments of coronary arteries were analyzed by near-infrared

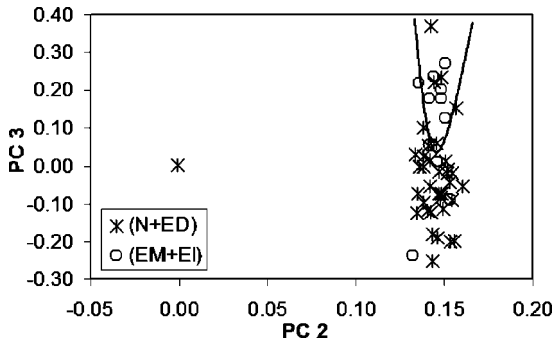

Fig. 5 Scatter plot of the second and third PC scores calculated using 48 FT-Raman spectra of human carotid arteries histopathologically classified as non-atherosclerotic. N+DTh represent normal tissue and discrete diffuse thickening of the intima layer and MTh+ITh represent moderate and intense diffuse thickening of the intima layer. Black line represents Mahalanobis-based classification surface.

Table 2 Results from diagnostic algorithm based on the scores of the PC2 and PC3 versus histopathology applied to 48 spectra nonatherosclerotic carotid arteries. N+DTh—normal+discrete diffuse thickening of the intima layer, MTh+Ith—moderate diffuse thickening and intense diffuse thickening of the intima layer.

	PCA diagnosis				
	N+ DTH	MTH+ ITH	Total	Sensitivity (%)	Specificity (%)
Histopathological diagnosis					
Normal+discrete diffuse thickening of the intima layer	32	5	37		
Moderate+intense diffuse thickening of the intima layer	3	8	11	86	73

Raman spectroscopy, with 95 samples correctly classified (87% agreement) leaving to high sensitivity and specificity values.

It has been found that alterations of diffuse thickening of the intima layer could be detected with FT-Raman spectroscopy. The analysis of arterial tissues with thickening using the PCA technique allowed the classification of normal arteries, discrete, moderate, and intense diffuse thickening of the intima layer into two categories: (1) normal and discrete diffuse thickening and (2) moderate and intense thickening. The sensitivity and specificity indices for diagnosis of diffuse thickening of the intima layer were 86% and 73%, respectively.

It has been shown that FT-Raman is capable of identifying and classifying the types of tissues found in the atherosclerotic process, and alterations in the diffuse thickening of the intima layer. Using FT-Raman spectroscopy it has been experimentally verified that one can get histochemical information about the composition of human carotid artery. FT-Raman spectrum not only discriminates between healthy and pathological artery wall with molecular specificity, but also provides an exclusive diagnostic signature for each tissue. Raman spectroscopy can go further, with identification of nonatherosclerotic thickening of the artery wall, revealing an important condition not identified so far. Raman technique could also enable the study of atherogenesis *in situ*, or even the evolution of arterial thickening, allowing the investigation of the disease progression as well as the response of different therapeutic modalities. These results suggest that Raman spectroscopy may be turned into a promising diagnostic technique in therapeutics.

Acknowledgments

One of the authors (A.A.M.) thanks CNPq, Grant No. 302393/2003-0 and FAPESP (Research Support Foundation of São Paulo State), Grant No. 01/14384-8 for financial support.

References

1. R.S. Cotran, V. Kumar, and T. Collins, *Patologia Estrutural e Funcional*, 6th ed., pp. 441–485, Guanabara Koogan, Rio de Janeiro, RJ (2000).
2. E. Braunwald, *Tratado de Medicina Cardiovascular*, 5th ed., pp. 1179–1200, Editora Roca LTDA., São Paulo-SP (1999).
3. H.C. Stay, ''Evolution and progression of atherosclerotic lesions in coronary arteries in children and young adults,'' *Arteriosclerosis Suppl* **9**(1), I19–I32 (1989).
4. E. Rubin and J.L. Farber, *Patologia*, pp. 402–441, Editora Interlivros Edições Ltda., Rio de Janeiro, RJ (1990).
5. C. Kittrell, R.L. Willett, C. de los Santos-Pacheco, N.B. Ratliff, J.R. Kramer, E.G. Malk, and M.S. Feld, ''Diagnosis of fibrous arterial atherosclerosis using fluorescence,'' *Appl. Opt.* **24**, 2280–2281 (1985).
6. M. Keijzer, R. Richards-Kortum, S.L. Jacques, and M.S. Feld, ''Fluorescence spectroscopy of turbid media: Autofluorescence of human aorta,'' *Appl. Opt.* **28**(20), 4286–4292 (1989).
7. F. Bosshart, U. Utzinger, O.M. Hess, J. Wyser, A. Mueller, J. Schneider, P. Niederer, M. Anliker, and H.P. Krayenbuehl, ''Fluorescence spectroscopy for identification of atherosclerotic tissue,'' *Cardiovasc. Res.* **26**(6), 620–625 (1992).
8. L.I. Deckelbaum, S.P. Desai, C. Kim, and J.J. Scott, ''Evaluation of a fluorescence feedback system for guidance of laser angioplasty,'' *Lasers Surg. Med.* **16**(3), 226–234 (1995).
9. A.J. Morguet, R.E. Gabriel, A.B. Buchwald, G.S. Werner, R. Nyga, and H. Kreuzer, ''Single-laser approach for fluorescence guidance of excimer laser angioplasty at 308 nm: Evaluation *in vitro* and during coronary angioplasty,'' *Lasers Surg. Med.* **20**(4), 382–393 (1997).
10. P. Weinmann, M. Jouan, N.Q. Dao, B. Lacroix, C. Groiselle, J.P. Bonte, and G. Luc, ''Quantitative analysis of cholesterol and cholesteryl esters in human atherosclerotic plaques using near-infrared Raman spectroscopy,'' *Arteriosclerosis (Dallas)* **140**, 81–88 (1998).
11. T.J. Römer, J.F. Brennan III, M. Fitzmaurice, M.L. Feldstein, G. Deinum, J.L. Myles, J.R. Kramer, R.S. Lees, and M.S. Feld, ''Histopathology of human coronary atherosclerosis by quantifying its chemical composition with Raman spectroscopy,'' *Circulation* **97**, 878–885 (1998).
12. G. Deinum, D. Rodriguez, T.J. Römer, M. Fitzmaurice, J.R. Kramer, and M.S. Feld, ''Histological classification of Raman spectra of human coronary artery atherosclerosis using principal component analysis,'' *Appl. Spectrosc.* **53**(8), 938–942 (1999).
13. J.F. Brennan, T.J. Romer, R.S. Lees, A.M. Tercyak, J.R. Kramer, and M.S. Feld, ''Determination of human coronary artery composition by Raman spectroscopy,'' *Circulation* **96**(1), 99–105 (1997).
14. L. Silveira, Jr., S. Sathaiah, R.A. Zàngaro, M.T.T. Pacheco, M.C. Chavantes, and C.A.G. Pasqualucci, ''Correlation between near-infrared Raman spectroscopy and the histopathological analysis of aherosclerosis in human coronary arteries,'' *Lasers Surg. Med.* **30**(4), 290–297 (2002).
15. R.R. Alfano, C.H. Liu, W.L. Sha, H.R. Zhu, D.L. Akins, J. Cleary, R. Prudente, and E. Cellmer, *Lasers Life Sci.* **4**, 23 (1991).
16. R. Manoharan, Y. Wang, and M.S. Feld, ''Histochemical Analysis of Biological Tissues using Raman Spectroscopy,'' *Spectrochim. Acta, Part A* **52**, 215–249 (1996).
17. P. Geladi and B.R. Kowalski, ''Partial least square regression: A tutorial,'' *Anal. Chim. Acta* **185**, 1–17 (1986).
18. E.B. Hanlon, I. Itzkan, R.R. Dasari, M.S. Feld, R.J. Ferrante, A.C. McKee, D. Lathi, and N.W. Kowall, ''Near-infrared fluorescence

spectroscopy detects Alzheimer's disease *in vitro*,'' *Photochem. Photobiol.* **70**(2), 236–242 (1999).
19. A. Mahadevan-Jansen, M.F. Mitchell, N. Ramanujam, A. Malpica, S. Thomsen, U. Utzinger, and R. Richards-Kortum, ''Near-infrared Raman spectroscopy for *in vitro* detection of cervical precancers,'' *Photochem. Photobiol.* **68**(1), 123–132 (1998).
20. R. Manoharan, K. Shafer, L. Perelman, J. Wu, K. Chen, G. Deinum, M. Fitzmaurice, J. Myles, J. Crowe, R.R. Dasari, and M.S. Feld, ''Raman spectroscopy and fluorescence photon migration for breast cancer diagnosis and imaging,'' *Photochem. Photobiol.* **67**(1), 15–22 (1998).
21. L.O. Nunes, A.A. Martin, L.J. Silveira, and M. Zampieri, ''FT-Raman spectroscopy study for skin cancer diagnosis,'' *Spectroscopy-An International Journal* **17**(2–3), 597–602 (2003).
22. E.J. Ciaccio, S.M. Dunn, and M. Akay, ''Biosignal pattern-recognition and interpretation systems,'' *IEEE Eng. Med. Biol. Mag.* **13**, 129–135 (1994).
23. H.C. Stary, A.B. Chandler, R.E. Dinsmore, V. Fuster, S. Glasgov, and W. Insull, et al. ''A definition of advanced types of atherosclerotic lesions and a histological classification of atherosclerosis— A Report from the Committee on Vascular-Lesions of the Council on Atherosclerosis,'' *Circulation* **92**(5), 1355–1374 (1995).
24. R. P Rava, J. J Baraga, and M. S. Feld, ''Near-infrared Fourier-transform Raman-spectroscopy of human artery,'' *Spectrochim. Acta, Part A* **47**, 509–512 (1991).
25. J.F. Brennan, ''*Near infrared Raman spectroscopy for human artery histochemistry and histopathology*,'' PhD thesis, Massachusetts Institute of Technology, 1995, Cambridge, MA, p. 106.
26. N.S. Weiss, ''*Diagnostic and screening test: What information is needed before developing a policy for their use*?'' in: *Clinical Epidemiology: The Study of the Outcome of Illness*, pp. 15–32, Oxford University Press, New York, (1986).